Available online at www.sciencedirect.com
ScienceDirect
Journal of Power Sources 167 (2007) 413–419
JOURNAL OF POWER SOURCES
www.elsevier.com/locate/jpowsour

Electrocatalytic properties improvement on carbon-nanotubes coated reaction surface for micro-DMFC

Shou-Kai Wang [a], Fangang Tseng [a,b,c], Tsung-Kuang Yeh [b], Ching-Chang Chieng [a,b,*]

[a] *Institute of Microelectromechanical System, National Tsing Hua University, Hsinchu 30043, Taiwan*
[b] *Department of Engineering and System Science, National Tsing Hua University, Hsinchu 30043, Taiwan*
[c] *Division of Mechanics, Research Center for Applied Sciences, Academia Sinica, Taiwan, ROC*

Received 8 November 2006; received in revised form 16 February 2007; accepted 19 February 2007
Available online 2 March 2007

Abstract

In this paper, the enhancement of electrocatalytic performance of carbon nanotubes (CNTs) grown on silicon substrate was demonstrated as compared with the conventional reaction surfaces including bare silicon wafer, carbon cloth and carbon paper, and all were with a thin Pt film (10 nm) coating. The peak current density was doubled by the Pt film/CNTs electrode comparing to Pt film/carbon cloth and about six times comparing to silicon wafer because of the large reaction surface area and excellent CO_2 microbubble removal capability by the CNTs nanostructure. The results indicated that the electrocatalytic performance of catalyst was significantly improved for the peak current density on better linear relationship to methanol concentration and square root of sweeping-rate, better exponential relationship to temperature and higher peak current density on different substrate tiling angles, which greatly attribute to the rapid microbubbles removal on nanostructured hydrophilic CNTs surface. These conclusions can be taken as references to designing micro-DMFC in the future.

Keywords: Electrocatalytic activity; Carbon-nanotubes; Micro-DMFC; Bubble removal

1. Introduction

The direct methanol fuel cell (DMFC) is a promising power source for portable applications due to its simple handling and processing of fuel and low total operating cost [1]. The performance of DMFC has been remarkably improved in the past years, but the poisoning of the catalyst [2,3], fuel crossover [4], CO_2 bubbles collection [5,6] and lack of reactive surface area [7], etc., are still the issues of interest. The structure of the carbon supports for catalyst layer have been demonstrated to improve the catalytic activity by increasing the number of catalytically active sites, such as carbon black [8,9], carbon-nanotubes [10,11], nanofibres [12,13], onion-like fullerenes [14] and ordered mesoporous carbon (OMC) [15–18]. For the fuel cell applications, carbon supports also have additional functions as methanol crossover reduction [19] and water handling capability for removing water generated at the cathode.

The issues of CO_2 bubbles collection and being lack of reactive surface area are related to the bubble generation/departure and the resultant activity of catalyst. If the bubbles are trapped on the electrode surface, the reaction area will be covered and isolated by the bubbles along with the reduction of cell performance. The implantation of nanostructure carbon nanotubes (CNTs) not only increases the catalytically active sites but also can affect surface tension and friction forces on microbubbles by the increased surface area. In this study, implanted CNTs on substrates have been proposed to speed-up the bubble removal which has demonstrated in a separate paper [20] as well as increase the reaction area for catalytic properties enhancement of the catalyst. In addition, a platinum film is deposited on the CNTs by E-Beam evaporator to enhance catalytic activity by the high dispersion of nanosized Pt particles. Furthermore, the electrocatalytic property of the surface with implanted CNTs substrates are compared with those of conventional substrates such as bare silicon wafer, carbon cloth or carbon paper. All substrates are

* Corresponding author at: Department of Engineering and System Science, National Tsing Hua University, Hsinchu 30043, Taiwan. Tel.: +886 3 5716691; fax: +886 3 5720724.
E-mail address: cchieng@ess.nthu.edu.tw (C.-C. Chieng).

0378-7753/$ – see front matter © 2007 Elsevier B.V. All rights reserved.
doi:10.1016/j.jpowsour.2007.02.057

covered with a ~10 nm Pt film which is deposited with E-beam evaporator for the studies of electrocatalytic mechanism during the methanol oxidation process.

2. Experimental setup

In order to demonstrate the effect of CNT implantation, there were key works to conduct: electrode fabrication and pretreatment and the electrochemical measurement.

2.1. Electrodes fabrication process

The fabrication processes of electrodes with different substrates are shown in Fig. 1. The substrates in this study included silicon wafer (500 μm in thickness), carbon paper, carbon cloth and CNTs. Except CNTs, all the substrates were coated with a titanium film (100 nm in thickness) and qa platinum film (~10 nm in thickness) by E-beam physical vapor deposition. The titanium film served as an adhesion layer and an electrode, and the platinum film acted as a catalyst layer. A platinum film of ~10 nm was coated on substrates by E-beam physical vapor deposition, and the thickness could not be controlled but might be estimated by the approximate loading and transmission electron microscopy (TEM) images. It was found that platinum nanoparticles were formed and occupied 1/4 of CNTs surface with an estimated load of ~0.14 mg cm^{-2}, while the Pt loading on flat substrate is estimated 2.145 mg cm^{-2}. All four substrates are loaded with Pt under the same E-beam evaporation condition.

CNTs were grown directly on silicon wafer by thermal chemical vapor deposition technique in a tube furnace. Nickel was deposited by E-beam physical vapor deposition as the catalyst for the growth of CNTs. Because of the poor bonding between nickel and silicon wafer, the 100 nm titanium film was deposited as the adhesion layer and electrode by E-beam evaporator. In order to anneal catalyst film (Ni) to form nanoparticles and to decompose the ethylene gas (C_2H_4) which was the source of carbon, the environmental temperature was maintained at 800 °C during the growth process of CNTs. Argon (200 sccm) and ammonia (200 sccm) were loaded into the tube furnace for 10 min first to reduce metal catalyst. Then ethylene gas was loaded into the tube furnace with a flow rate of 30 sccm for 5 min. Finally a 10 nm Pt film was deposited on the prepared CNTs by E-beam evaporation. The grown CNTs and Pt film/CNTs were examined by scanning electron microscopy (SEM) and TEM as shown in Fig. 2. According to Fig. 2, the CNTs were randomly curved with diameters of 100–150 nm and an average height of ~2 μm (Fig. 2b). Conformation of CNTs shown in Fig. 2c indicated the unchanged and undamaged CNTs after the deposition of platinum particles. Pt nanoparticles with diameters ranging from 5 to 15 nm are revealed by TEM in Fig. 2d.

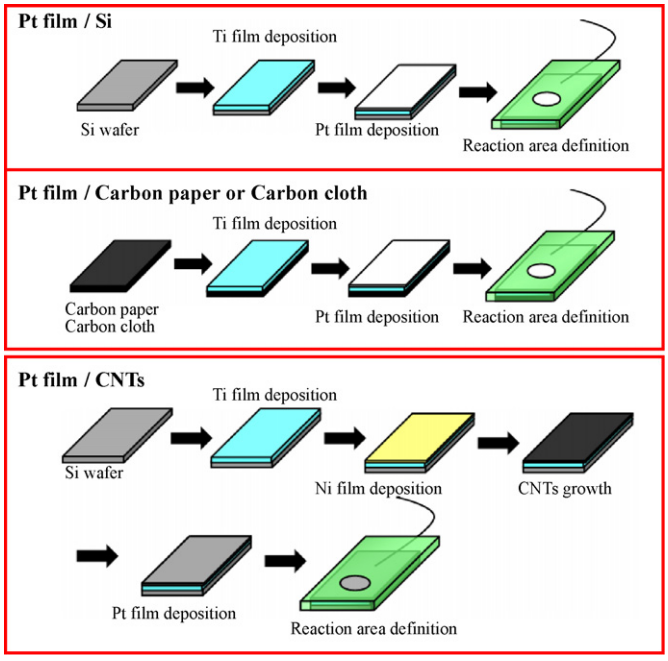

Fig. 1. The fabrication process of electrodes with different substrates.

2.2. Pretreatment of electrodes

To enhance the hydrophilic property and electrochemical activity of the electrode surface, the Pt-coated electrodes were simply immersed in a 30% hydrogen peroxide aqueous solution for 3–4 min and then rinsed in deionized (DI) water and dried in air before electrocatalytic tests. The contact angle of the electrode surface was modified lower than 20°, as shown in Fig. 3, for the surfaces of Pt film/Si, Pt film/CNTs, Pt film/carbon paper and Pt film/carbon cloth. The hydrophilic treatment removed the gas film on the electrodes to enhance the electrochemical reaction. The thin platinum coating (~10 nm) did not affect the surface morphology formed by CNTs.

2.3. Electrochemical measurement

A standard three-electrode cell, as shown in Fig. 4, was employed for electrochemical measurement. The sample with a definite area of 0.2 cm^2, a platinum wire and a Ag/AgCl electrode with 1N KCl electrolyte were employed as the working electrode, counter electrode and the reference electrode, respectively. Cyclic voltammetry (CV, potential sweeping range: −0.2 V to 1 V) and potentiostatic method (0.8 V in present work) in 1 M CH_3OH + 0.5 M H_2SO_4 aqueous solutions were applied to measure electrocatalytic properties. All experiments were carried out at 27 °C under atmospheric pressure except for the methanol concentration test (35 °C) and long-term stability test (30 °C). All chemicals were purchased at reagent grade and DI water was used throughout.

3. Results and discussion

3.1. Electrocatalytic performance of H_2O_2 pretreated Pt film

The contact angle and Faradyaic current density on Pt film surface were varied after the H_2O_2 pretreatment (Fig. 5).

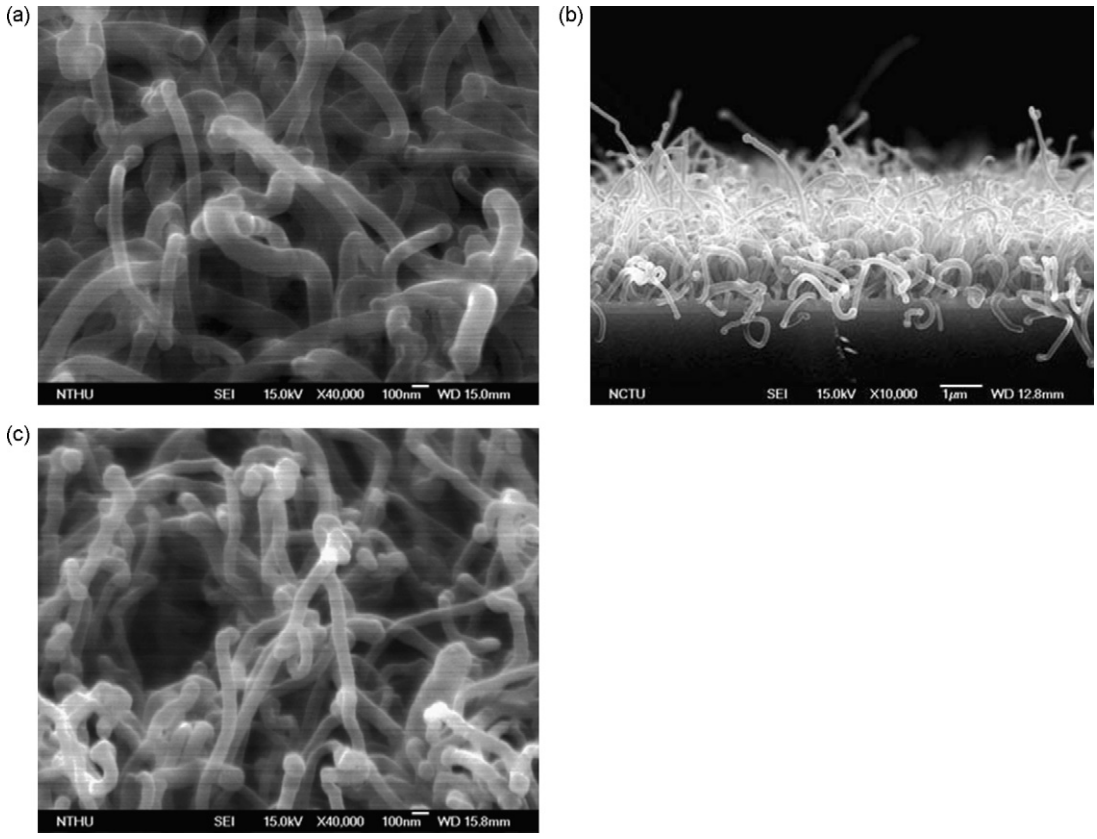

Fig. 2. The SEM images of CNTs (a) top view (40,000×), (b) lateral view (10,000×) and (c) Pt film/CNTs (top view, 40,000×).

For surfaces of Pt film/CNTs, Pt flim/carbon cloth and Pt film/carbon paper, the hydrophilic property (17°) returned back to its original hydrophobic degree (82°) 4 h after the pretreatment. The Faradyaic current density after pretreatment (1.65×10^{-4} A cm^{-2}) dropped to the original level of 0.2×10^{-4} A cm^{-2}, too. Strong oxidation property of H_2O_2 activated the catalytic site and clean away the impurities on the surface. Additionally, the hydrophilic nature allows much easier contact of the reactants with the catalytic sites. According to Wei et al. [21], an intermediate species of CH_2OH + Pt may be present during the course of methanol oxidation on pure Pt, and the reaction proceeds is

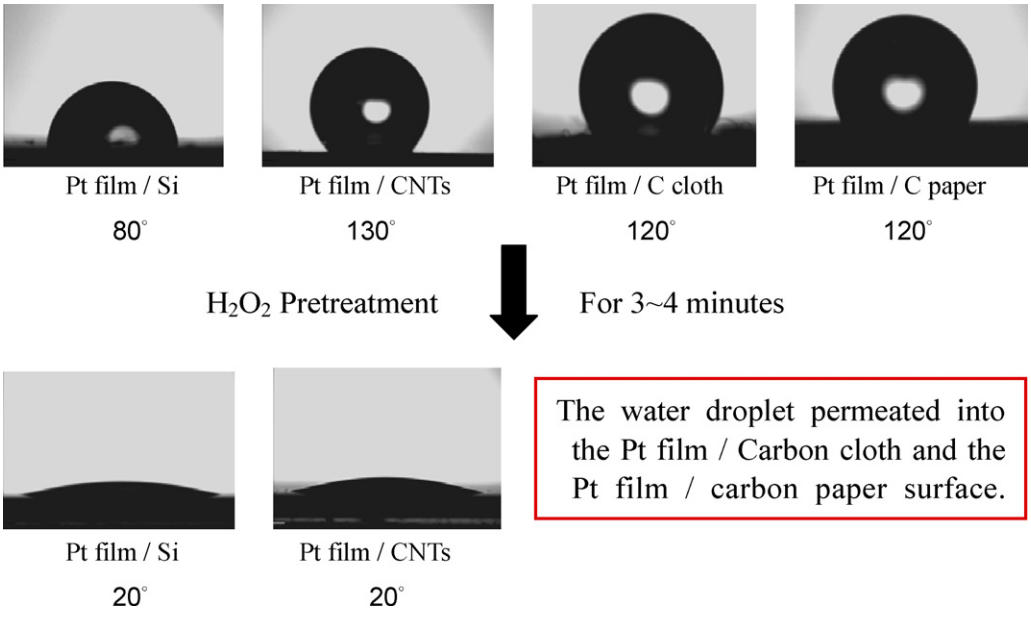

Fig. 3. The photo images of the contact angles on different electrode surfaces.

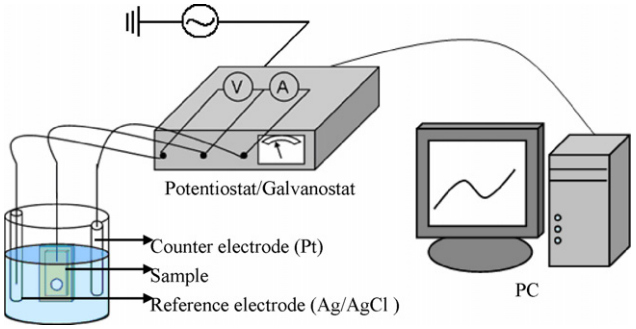

Fig. 4. The schematic diagram of electrochemical measurement system.

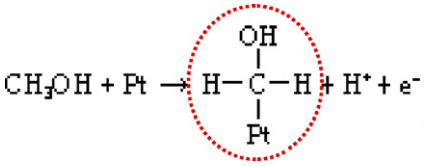

In the presence of oxide-rich surface on the Pt film, it was speculated that the intermediate species might further react with platinum oxide (Pt–O) by way of

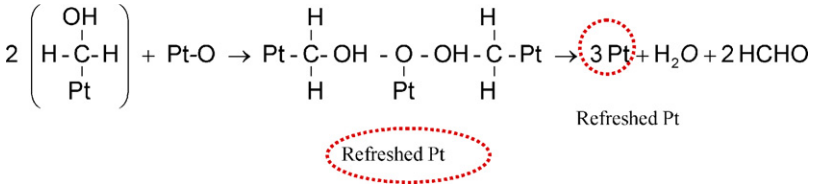

In terms of the reactions above, the Pt catalyst circled was refreshed by the reaction and then catalyzed methanol oxidation in a traditional manner. Because the Pt-oxides were eventually reduced to refreshed Pt atoms, the catalytic efficiency of these atoms raised enormously. The discussions above were the major reasons on catalytic current enhancement of H_2O_2 pretreated Pt film. However, the consumption of Pt–O reduced the activity from H_2O_2 led to the reduction of the production and the catalytically activity of refreshed Pt and thus the current eventually reduced as shown in Fig. 5. All of the experiments in the following sections were conducted 1–2 h before the consumption of the active Pt species.

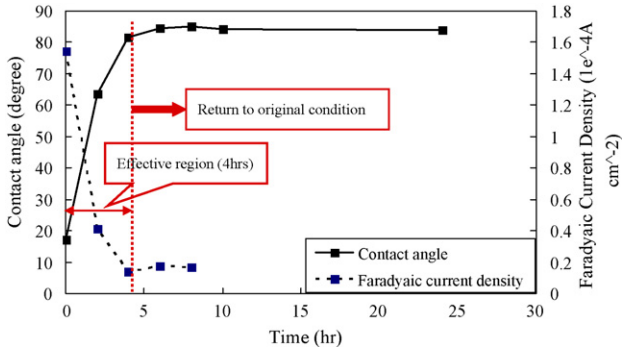

Fig. 5. Effect of H_2O_2 pretreatment on contact angle and Faradyaic current density vs. time for electrode of Pt film/Si. The ambient temperature is at 27 °C.

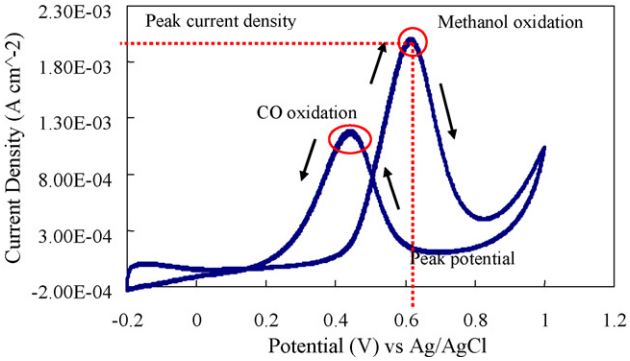

Fig. 6. The typical cyclic voltammogram in 1 M CH_3OH + 0.5 M H_2SO_4 aqueous solutions for electrode of Pt film/Si. The sweeping rate of CV is 50 mV s^{-1} and the ambient temperature is at 27 °C.

3.2. Electrocatalytic performance enhancement using CNTs implantation

Electrocatalytic performance of Pt catalyst was obtained by performing cyclic voltammetry in 1 M CH_3OH + 0.5 M H_2SO_4 aqueous solutions to yield a typical cyclic voltammogram in Fig. 6. Two oxidation peaks in the cyclic voltammogram were observed and they were corresponding to the potentials ranging from 0.6 to 0.7 V and 0.4 to 0.5 V, respectively. Electrocatalytic properties of Pt film measured by cyclic voltammetry in 1 M CH_3OH + 0.5 M H_2SO_4 aqueous solutions were characterized by the peak current density and the peak potential from the oxidation of methanol in Fig. 6. The peak current density for different substrates suggested that the performance be doubled by the Pt film on CNTs electrode comparing to Pt film/carbon cloth and about six times comparing to Pt film on Si because of the large reaction surface area (Fig. 7). Parallel study [20] of bubble

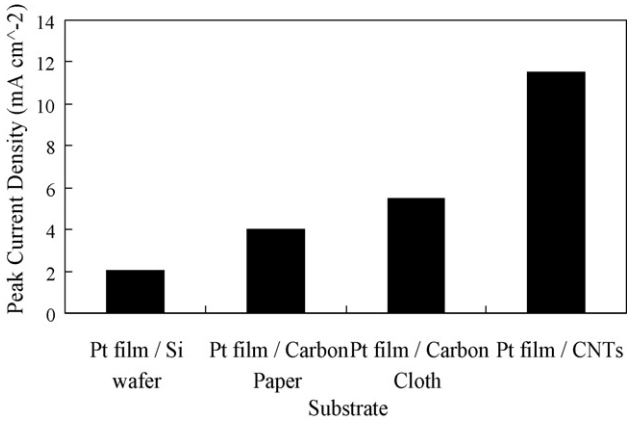

Fig. 7. The comparison of the peak current density in 1 M CH_3OH + 0.5 M H_2SO_4 aqueous solutions on different substrates. The sweeping rate of CV is 50 mV s^{-1} and the ambient temperature is at 27 °C.

departure from these surfaces indicated that much smaller bubble departure sizes for surface with grown CNTs and much higher bubble rising velocity for vertically grown CNTs on surfaces. Furthermore, electrochemical experiments had been performed to correlate the bubble generation and the resultant current on surfaces with implanted carbon-nanotubes.

These results revealed that excellent CO_2 microbubble removal capability by nanostructure of CNTs were one of the major causes of the enhancement.

3.3. Comparison of electrocatalytic properties

The enhancement of electrocatalytic properties using carbon-nanotubes (CNTs) to carry platinum (Pt) thin film for different substrates was demonstrated in terms of methanol concentration, sweeping rate, operating temperature and tilt angle of electrode surface. The effects of methanol concentration on electrocatalytic properties of Pt film on CNTs and Pt film on Si electrodes are shown in Figs. 8 and 9. Fig. 8 indicates that the peak current density of both electrodes was increased with the increase of methanol concentration as the environmental temperature was raised to 35 °C.

In the high concentration (>1 M) region, the relation between peak current density and methanol concentration of Pt film/CNTs was more linear than that of Pt film/Si. In other words, less decay of peak current density with methanol concentration for Pt film/CNTs electrode as compared with that for Pt film/Si was obtained, which implied that the electro catalytic

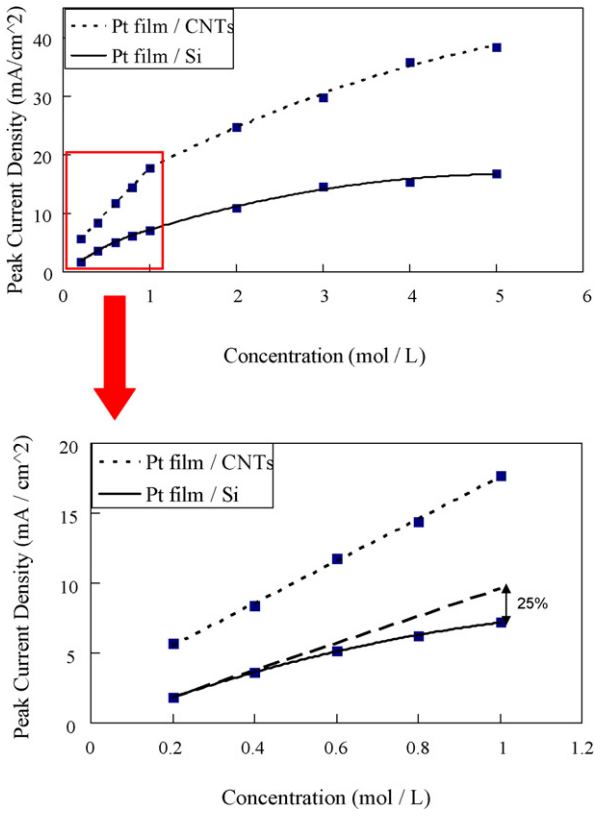

Fig. 8. Effect of methanol concentration on peak current density. The sweeping rate of CV is 50 mV s^{-1}. The ambient temperature is at 35 °C.

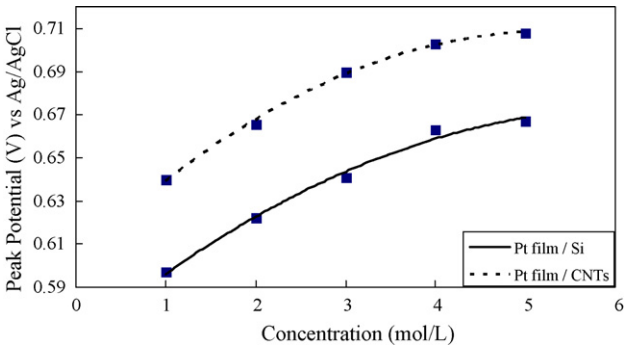

Fig. 9. Effect of methanol concentration on peak potential. The sweeping rate of CV is 50 mV s^{-1}. The ambient temperature is at 27 °C.

mechanism was affected by the trap of CO_2 microbubbles [20] and by the diffusion control of the methanol and the intermediates produced during the methanol oxidation. The explanation can be made by the following equation [22]:

$$I_p = (2.99 \times 10^5) n(\alpha n_a)^{1/2} A D^{1/2} C \nu^{1/2} \quad (1)$$

which is valid for irreversible systems, and I_p is the peak current, n the charge number, α the transfer coefficient, n_a the electron-transfer number of the rate determining step and ν is the sweeping rate of CV. In our system, all parameters in this equation except surface area (A) and diffusion coefficient (D) are constants as methanol concentration is varied. Since the surface area (A) and diffusion coefficient (D) in Eq. (1) are decreased with increased methanol concentration (C), relation of current density and concentration cannot be linear for both electrodes (Fig. 8a). However, on the Pt film/CNTs surface in reality, the phenomena of very small microbubble coverage on catalytic sites and very small decrease of reaction surface area occurred as methanol concentration increased, so the relationship of current density and methanol concentration for Pt film/CNTs was much more linear than that for Pt film/Si.

In the low concentration (<1 M) region, the diffusion coefficient maintains constant, and the peak current density is related to bubble coverage only. This was revealed by the linear relationship between peak current density and concentration of Pt film/CNTs electrode. From Fig. 8b, 25% loss was observed for Pt film/Si electrode at methanol concentration of 1 M due to microbubbles collection.

Since a higher methanol concentration implies a larger electrocatalytic current density and leads to more active sites of the Pt catalyst to be poisoned a higher peak potential is needed to drive electrocatalytic reaction. Thus, peak potential increased as methanol concentration increased (Fig. 9). Furthermore, because a higher electrocatalytic reaction efficiency leads to more CO poisoning on the Pt film/CNTs electrode, a higher peak potential from Pt film/CNTs than from Pt film/Si was obtained in Fig. 9.

Fig. 10 indicates that the peak current density of both electrodes was increased with square root of scan rate ($\nu^{1/2}$). The higher the scan rate was, the more reaction products were accumulated in the vicinity of the Pt film/Si electrode surface. Accordingly, the adsorption of methanol molecules decreased,

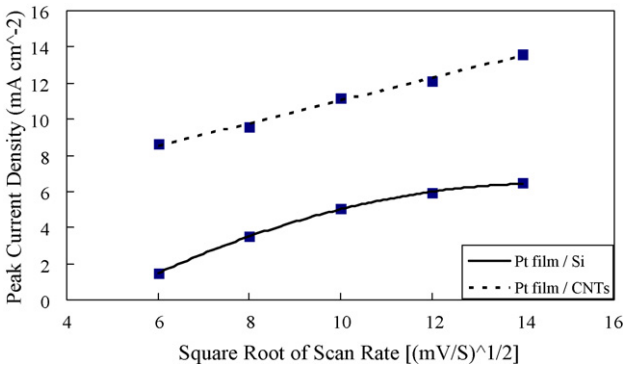

Fig. 10. Effect of square root of forward CV scan rate on peak current density obtained in 1 M CH_3OH + 0.5 M H_2SO_4 aqueous solutions. The ambient temperature is at 27 °C.

i.e. accumulation of reaction product (CO_2 microbubble) near electrode surface became more critical at higher reaction rate, and the reaction surface area was decreased, so as the non-linear relationship of square root of scan rate versus current density for Pt film/Si electrode was obtained. It also indicated that the linear dependence of square root of sweeping rate on the peak current density for the chip with implanted CNTs, which implied the constant active area most probably due to the fast removal of microbubbles with very small portion of the electrode covered by the microbubbles.

Fig. 11 shows that the peak current densities of both electrodes were increased with the temperature increase although more products (CO_2) were produced during methanol oxidation at higher temperature. It can be explained by the enormous raises of the catalyst activity, the diffusion coefficient and the reaction rate as temperature increases [6]. The reaction rate and temperature can be related by the following equation [25]:

$$\text{Reaction rate} \propto \exp\left(-\frac{E_{act}}{RT}\right) \quad (2)$$

where E_{act} is the activation energy, R the universal gas constant and T is the temperature (K). However, on the surface of Pt film/Si electrode, a great deal of reaction products (e.g. CO_2) and intermediates were accumulated during the electrocatalytic reaction and this accumulation phenomenon became more serious at higher temperatures due to higher reaction rates. Thus the peak current density could not be increased exponentially with temperature and the electrocatalytic efficiency was thus deteriorated as shown in Fig. 11. For the Pt film/CNTs electrode, the collection of CO_2 microbubbles was highly unlikely during the process with a fast bubble removal tendency, and the electrocatalytic reaction was only influenced by accumulation of intermediates, which led to exponential dependence between peak current and temperature in Fig. 11. Furthermore, an increasing peak current density of CO oxidation was also observed as the temperature was increased, implying that the degree of CO poisoning was increased at a higher temperature.

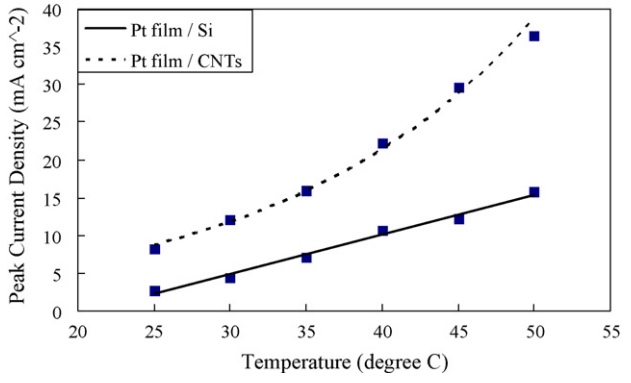

Fig. 11. Effect of temperature on peak current density obtained in 1 M CH_3OH + 0.5 M H_2SO_4 aqueous solutions. The sweeping rate of CV is 50 mV s^{-1}. The ambient temperature is at 27 °C.

According to Tseng et al. [20], microbubbles removal capability was different if the electrode surface was lay at a tilt angle with respect to horizontal plane (vertical to gravity). In addition to smaller bubbles departure radius and higher bubble removing velocity were observed for Pt film/CNTs electrode and for Pr film/Si electrode was observed, bubble departure radius were increased with increasing tilt angle of electrode up-facing surface, the peak current density was largely reduced as tilt angle was increased (Fig. 12). Because microbubbles coverage on Pt film/Si surface was much more serious than that on Pt film/CNTs surface, 68% loss of peak current density for Pt film/Si electrode was obtained but 25% loss was observed on Pt film/CNTs electrode as tilt angle was increased from 0° to 135°.

3.4. Long-term stability of catalytic performance on the Pt film/CNTs electrode

Fig. 13 plots the long-term stability of catalytic performance on the Pt film/CNTs electrode, indicating a gradual decrease in peak current density with increases in cycle number. At the 385th cycle, 38.9% loss of peak current density was observed. The explanations of this phenomenon were catalytic sites poisoned by CO molecules during the sweeping process [23], methanol

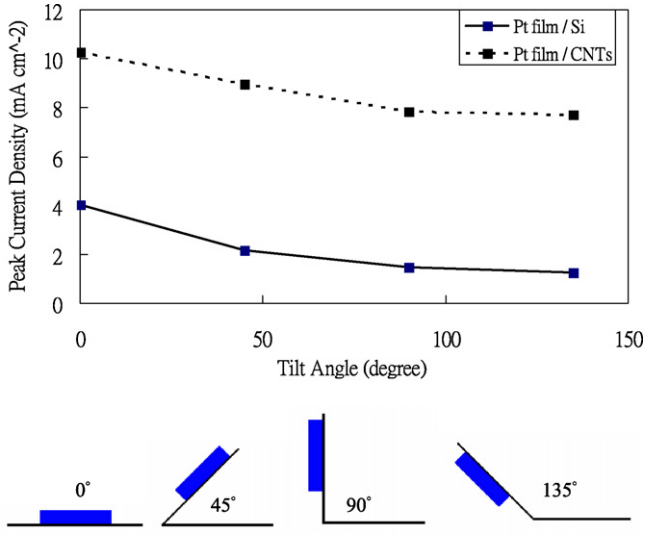

Fig. 12. Effect of tilt angle of electrode surface on peak current density obtained in 1 M CH_3OH + 0.5 M H_2SO_4 aqueous solutions. The sweeping rate of CV is 50 mV s^{-1} and the ambient temperature is at 27 °C.

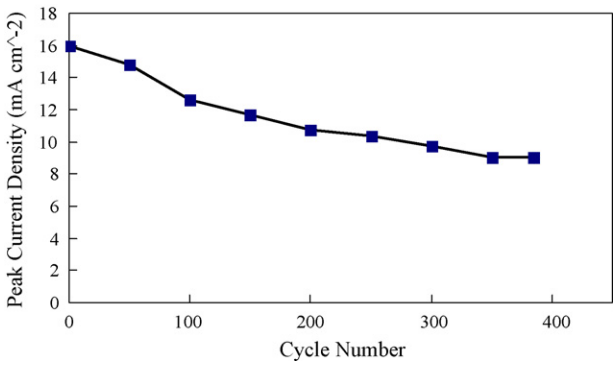

Fig. 13. Long-term stability of the Pt film/CNTs electrode obtained in 1 M CH_3OH + 0.5 M H_2SO_4 aqueous solutions. The sweeping rate of CV is 50 mV s^{-1} and the ambient temperature is at 30 °C.

molecules consumed by catalytic reaction, and change of the surface structure of Pt catalyst [24]. This CO poisoning effect can be further improved by the composition of Pt with other materials such Ru, which is out of the scope of the current paper.

4. Conclusion

The electrocatalytic performance by implantation of CNTs with Pt film (10 nm) coating were highly enhanced as compared with that on conventional substrates of bare silicon wafer, carbon cloth and carbon paper. The CNTs was shown as the best support material for Pt catalyst in these four substrates because of the largest peak current density due to the large surface area and excellent CO_2 microbubble removal. The peak current density versus temperature and square root of scan rate indicated that diffusion of intermediates and product collection during methanol oxidation on the electrode surface played an important role in the reaction process. Based upon the influences of methanol concentration, sweeping rate, operating temperature and tilt angle of electrode surface on the electrocatalytic properties of the electrodes, it was concluded that the Pt film/CNTs electrode led to a higher electrochemical reactivity due to faster microbubbles removal.

Acknowledgements

This work was supported by National Science Council under contract NSC-94-2218-E-007-017. Help from Mr. Hsien-Chih Peng and Mr. Chih-Hao Hsu on grown CNTs are highly appreciated.

References

[1] J.-H. Wee, J. Power Sources 161 (2006) 1–10.
[2] J.-M. Leger, J. Appl. Electrochem. 31 (2001) 767.
[3] L.D. Burke, M.A. Horgan, L.M. Hurley, L.C. Nagle, A.P. O'Mullane, J. Appl. Electrochem. 31 (2001) 729.
[4] B. Yang, A. Manthiram, Electrochem. Commun. 6 (2004) 231.
[5] P. Argyropoulos, K. Scott, W.M. Taama, J. Appl. Electrochem. 29 (1999) 661.
[6] H. Yang, T.S. Zhao, Q. Ye, J. Power Sources 139 (2005) 79.
[7] M.R. Shivhare, R.G. Allen, K. Scott, A.J. Morris, E.B. Martin, J. Electroanal. Chem. 595 (2006) 145–151.
[8] F. Cloaguen, J. Leger, C. Lamy, J. Appl. Electrochem. 27 (1997) 1052.
[9] C.H. Park, M.A. Scibioh, H.-J. Kim, I.-H. Oh, S.-A. Hong, H.Y. Ha, J. Power Sources 162 (2006) 1023–1028.
[10] S.H. Joo, S.J. Choi, I. Oh, J. Kwak, Z. Liu, O. Terasaki, R. Ryoo, Nature 412 (2001) 169.
[11] G. Che, B.B. Lakshmi, E.R. Fisher, C.R. Martin, Nature 393 (1998) 346.
[12] C.A. Bessel, K. Laubernds, N.M. Rodriguez, et al., J. Phys. Chem. B 105 (2001) 1115.
[13] E.S. Steigerwalt, G.A. Deluga, C.M. Lukehart, J. Phys. Chem. B 106 (2002) 760.
[14] B. Xu, X. Yang, X. Wang, J. Guo, X. Liu, J. Power Sources 162 (2006) 160–164.
[15] J. Ding, K.-Y. Chan, J. Ren, F.-S. Xiao, Electrochim. Acta 50 (2005) 3131.
[16] F. Su, J. Zeng, X. Bao, Y. Yu, J.Y. Lee, X.S. Zhao, Chem. Mater. 17 (2005) 3960.
[17] J.-H. Nam, Y.-Y. Jang, Y.-U. Kwon, J.-D. Nam, Electrochem. Commun. 6 (2004) 737.
[18] S.H. Joo, C. Pak, D.J. You, S.-A. Lee, H.I. Lee, J.M. Kim, H. Chang, D. Seung, Electrochim. Acta 52 (2006) 1618–1626.
[19] N. Nakagawa, M.A. Abdelkareem, K. Sekimoto, J. Power Sources 160 (2006) 105–115.
[20] F. Tseng, C. Pan, J.-H. Chuang, Y.-S. Wu, C.-C. Chieng, International Conference on Multiphase Flow ICMF 2007, Leipzig, Germany, July 9–13, 2007.
[21] Z. Wei, H. Guo, Z. Tang, J. Power Sources 58 (1996) 239.
[22] C.-C. Hu, Fundamentals and Methods of Electrochemistry, Wu-Nan Book Inc., Taiwan, 2002.
[23] J. Kua, W.A. Goddard III, J. Am. Chem. Soc. 121 (1999) 10928.
[24] L. Jiang, G. Sun, S. Wang, G. Wang, Q. Xin, Z. Zhou, B. Zhou, Electrochem. Commun. 7 (2005) 663–668.
[25] M. boyd, Organic Chemistry, Prentice-Hall Inc., 1992.